Highly loaded magnetocaloric $La(Fe,Si)_{13}H$ powder Composites for additive manufacturing: Characterization and Modeling of field-induced Phase Transition

L. Hirsinger , T. Barriere

Université de Franche-Comté, CNRS, Institut FEMTO-ST, 15b Avenue des Montboucons, F-25000 Besançon, France

Introduction

The gases used in current refrigeration systems are harmful to the environment (e.g. ozone depletion, greenhouse effect) [1-2]. An innovative and promising alternative is magnetic refrigeration based on the magnetocaloric effects (**MCE**) of solid alloys used in the form of regenerators [3]. Several prototypes of magnetocaloric (**MC**) regenerators have been built and show a high coefficient of performance (COP), but very few are on the market. These MC regenerators still have certain limitations, such as the brittleness of MC intermetallic alloys [4].

❑ Aims:

To develop and characterise a magnetocaloric composite highly loaded with magnetocaloric powder and based on polymer (PLA/LDPE + EVA + SA) by mixing dedicated to the 3D extrusion and additive manufacturing process / To carry out numerical simulations of the thermo-magnetic-mechanical coupling of the composite.

❑ Scientific challenges: The composite must have relevant magnetocaloric properties (ΔT_{ad} and ΔS_m) similar to the reference bulks materials (Gd, Gd derivative and Mn-Fe-Si-P).

where PLA denotes Polylactic Acid, LDPE Low - Density PolyEthylene, EVA Ethylene-Vinyl Acetate and SA Stearic Acid.

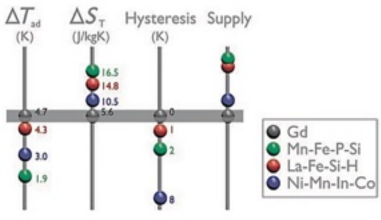

Classification of MC Materials with large MCE compared to Gd [5]

Elaboration, Shaping and Characterisation of MagnetoCaloric (or MC) Composites

Elaboration of highly loaded MC composites [6]:

Materials in powder form	Transition temperature (K)	Entropy variation (J/kg.K)
Gd	293	3 ± 1
$La(Fe,Si)_{13}H$	235	9-12 ± 1
$Ni_{50}Co_2Mn_{33}In_{15}$	298	5 ± 1

	Constituents of the binder: Polymers			Additives
Designation	Polylactic Acid (PLA)	Low - Density PolyEthylene (LDPE)	Ethylene-Vinyl Acetate (EVA)	Stearic Acid (SA)
Function	Dedicated to 3D printing	Dedicated to extrusion	Improves elasticity	Improves powder wettability

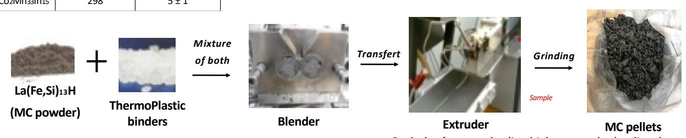

Optimized composite (i.e. highest powder loading, best suited for the elaboration and 3D printing processes):
Binder (47.5% LDPE + 47.5% EVA + 5%SA)
*+ **50 vol% of $La(Fe,Si)_{13}H$** powder (**88% by mass**).*

Shaping of MC composites:

- **Shaping by extrusion [7]:**

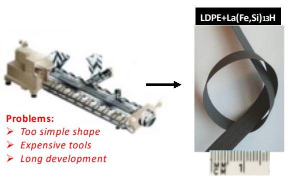

- **Shaping by 3D printing based on Pellets [8]:**

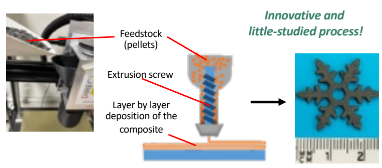

Structural analysis of the printed magnetocaloric composite [6]

(with optimized print settings: V = 10 mm/s, $Ø_{buse}$ = 8 mm, T = 413 K**):**

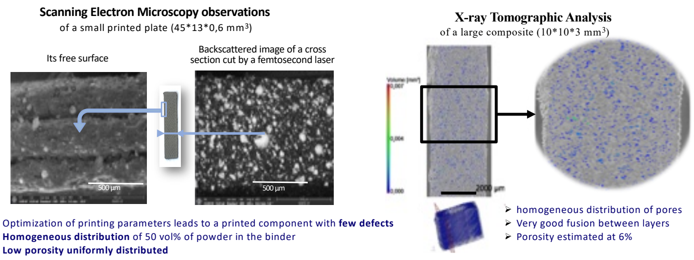

- Optimization of printing parameters leads to a printed component with **few defects**
- **Homogeneous distribution** of 50 vol% of powder in the binder
- **Low porosity uniformly distributed**
- homogeneous distribution of pores
- Very good fusion between layers
- Porosity estimated at 6%

Magnetocaloric characterization [6]:

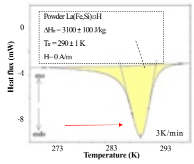

$$\Delta s = \frac{\Delta H_{tr}}{T_{tr}}$$

Evaluation of entropy variation Δs by DSC measurement

Materials	ΔH_{tr} (Jkg^{-1}) ± 100	Δs ($JK^{-1}kg^{-1}$) ± 0,1
Powder $La(Fe,Si)_{13}H$	3100	10,7
Printed composite	2700	9,3

Magnetocaloric evaluation criteria P_M

$$P_M = \frac{\Delta s_{composite\ per\ unit\ mass}}{\Delta s_{powder per\ unit\ mass}}$$

, if $P_M = Ø_{mass}$ then same quantity of heat released or absorbed as the powder alone.

Reference	Main binder	Mass fraction $Ø_{mass}$ of powder $La(Fe,Si)_{13}H$ (% by mass)	Transition temperature (K)	P_M (%)
J. Lanzarini et al. [7]	LDPE	92	293	92
Á. Díaz-García et al. [8]	PLA	55	289	45
This work	PLA	***88***	290	***87***

- Estimation close to the literature for $La(Fe,Si)_{13}H$ powder (~10 $JK^{-1}kg^{-1}$ between 0-1T)
- **High magnetocaloric properties of the composite** thanks to its high powder charge and translated by the P_M criterion
- The magnetocaloric effect of the composite respects a mixing law (i.e. proportional to the mass fraction of powder)

Modelling of field-induced Phase Transition in Ni-Co-Mn-In Single Crystal

Magnetization versus Temperature from [9]

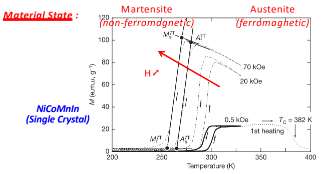

Figure 1 | Thermomagnetization curves of the $Ni_{45}Co_5Mn_{36.6}In_{13.4}$ alloy measured in several magnetic fields by the sample extraction method. The specimen quenched from 1,173 K was first measured during heating in H = 0.5 kOe from room temperature to 473 K followed by furnace cooling. The magnetization change due to martensitic transformation was cyclically measured in the temperature range from 330 K to 200 K in the following order: H = 0.5, 20 and 70 kOe. '1T' indicates values obtained at 7 tesla (=70 kOe).

Clausius-Clapeyron (or State) diagram from [12]

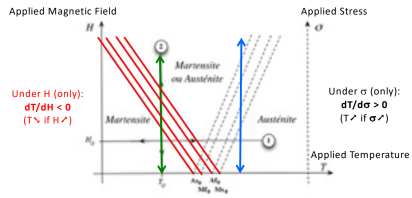

Phase Transformation induced by Stress σ : Pseudo-elasticity *(Well-known)*
For dT/dH > 0, Phase Transformation induced by Magnetic Field H
(Jeong et al., Mat. Eng. A359 (2003))
Reverse Phase Transformation induced by Stress σ *(Also well-known)*
For dT/dH <0, **Reverse Phase Transformation induced by magnetic field H**
= Meta-magnetic behaviour

Modeling of Phase Transformation induced by magnetic field, mechanical stress and variation of temperature

In the framework of Thermodynamics of Irreversible Processes [10-12],

- **Employed Variables**:

z : Volume fraction of Austenite

	State variables		Associated Forces
	Observable	Internal	
Thermal	T		$-s$
Mechanics	$\underline{\varepsilon}$	z	$\underline{\sigma}$ π^f
Magnetism	H		$-\mu_0 M$

- **Free Energy**:

$$\Phi(\underline{\varepsilon},T,z,\alpha) = \underbrace{\frac{1}{2}(\underline{\varepsilon}-\underline{\varepsilon}^{th}_{(T)}-\underline{\varepsilon}^{tr}_{(z)}):\underline{\underline{C}}:(\underline{\varepsilon}-\underline{\varepsilon}^{th}_{(T)}-\underline{\varepsilon}^{tr}_{(z)})}_{Elasticity} - \underbrace{K_{(z)}\,\underline{\sigma}^E:\Delta\underline{\varepsilon}^{tr}_{(z)}}_{Pseudo-Elastic\ Behavior}$$

$$\underbrace{-\mu_0\left[z\,\Delta M_{S(T)}+M_S^M\right]G_{(H)}}_{Magnetic\ Behavior} + \underbrace{z(\Delta s_V\,T-\Delta u_V)}_{Chemical} + \underbrace{C_a\left[(T-T_0)-T\ln\left(\frac{T}{T_0}\right)\right]}_{Thermal}$$

with the choice of the deformation tensor of Phase Transformation: $\underline{\varepsilon}^{tr}_{(z)} = (1-z)\,\underline{\gamma}^{tr}$

- **Driving Force π^{f*}**:

By putting each State Laws on the Dissipation expression, we identify the Thermodynamic Driving Force that exert on the interface between Martensite and Austenite as being:

$$\pi^{f*}_{(\underline{\sigma},H,T,z)} = \underbrace{\Delta\underline{\varepsilon}^{tr}:[\,\underline{\sigma}}_{Elasticity} - \underbrace{k_{(1-z)}\,\underline{\sigma}^E\,]}_{PEB} + \underbrace{\mu_0\Delta M_{S(T)}\,G(H)}_{Magnetism} + \underbrace{\Delta s_V\,T-\Delta u_V}_{Chemical}$$

The effect of Magnetism is proportional to the Applied Magnetic Field H and to the difference of Magnetization at Saturation of Austenite ΔMs.

- **Evolution law of variable z** :

By introducing a Yield Surface and by writing the Consistency Equation, we obtain the Evolution Law of the volume fraction z of the Austenite formed by Mechanical Stress, Magnetic Field and Temperature variation as being:

$$\dot{z} = \frac{dz}{dt} = \frac{\overbrace{\Delta\underline{\varepsilon}^{tr}:\dot{\underline{\sigma}}}^{Elasticity} + \overbrace{\mu_0\,\Delta M_{(H,T)}\,\dot{H}}^{Magnetism} + \overbrace{\left[\Delta s_V+\mu_0\,\Delta M'_{s(T)}\,G_{(H)}\right]\dot{T}}^{Chemical}}{-k'_{(1-z)}\,\Delta\underline{\varepsilon}^{tr}:\underline{\sigma}^E}$$

Temperature cycling: Experiment [13] & simulation

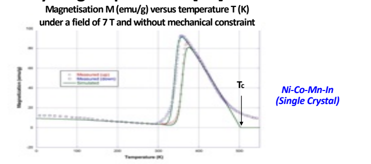

Meta-magnetic behavior: experimentation [13] and simulation

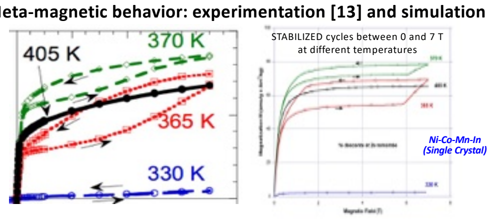

Entropy variation during a temperature cycling: Simulation

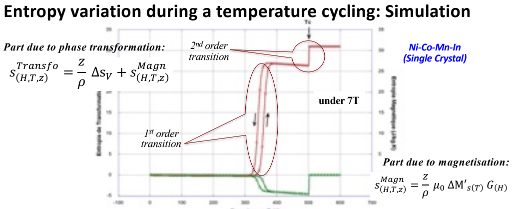

$$s^{Transfo}_{(H,T,z)} = \frac{z}{\rho}\,\Delta s_V + s^{Magn}_{(H,T,z)}$$

$$s^{Magn}_{(H,T,z)} = \frac{z}{\rho}\,\mu_0\,\Delta M'_{s(T)}\,G_{(H)}$$

References

[1] X. Hou et al., Journal of Alloys and Compounds. 646 **(2015)** 503-511
[2] V. Franco et al., Progress in Materials Science. 93 **(2018)** 112–232
[3] K.K. Nielsen et al., International journal of refrigeration. 34 **(2011)** 603-616
[4] T. Gottschall et al., Nature Materials. 17 **(2018)** 929–934
[5] A. Waske et al., MRS Bulletin, 43(04) **(2018)** 269–273
[6] K.D. N'dri et al., Powder Technology 425 **(2023)** 118616
[7] J. Lanzarini et al., J. of Materials Processing Tech. 273 **(2019)** 116244
[8] Á. Díaz-García et al., Composites Communications. 35 **(2022)** 101352
[9] R. Kainuma et al., Nature 439 **(2006)** 957
[10] L. Hirsinger et al., J. Phys. IV Proc. 112 **(2003)** 977-980
[11] L. Hirsinger, Phys. Status Solidi C 1, 12 **(2004)** 3458
[12] L. Hirsinger, Materials Today: Proc., 2 **(2015)** S597
[13] D. Bourgault et al., APL 96 **(2010)** 132501

Contacts
Laurent HIRSINGER (laurent.hirsinger@femto-st.fr)
Thierry BARRIERE (thierry.barriere@univ-fcomte.fr)

membres de UBFC
ISITE-BFC
ANR-15-IDEX-0003
COMPOMAG Project
(Innovative micro-structured magneto-caloric composites for sustainable and eco-friendly refrigeration machines and heat pumps).